International Journal of Mechanical Sciences 115-116 (2016) 1–11

Contents lists available at ScienceDirect

International Journal of Mechanical Sciences

journal homepage: www.elsevier.com/locate/ijmecsci

Experimental and theoretical investigation on transverse vibration of delaminated cross-ply composite beams

K. Torabi [a,*], M. Shariati-Nia [a], M. Heidari-Rarani [b]

[a] Department of Mechanical Engineering, University of Kashan, Kashan 8731751167, Iran
[b] Department of Mechanical Engineering, Faculty of Engineering, University of Isfahan, Isfahan 81746-73441, Iran

ARTICLE INFO

Article history:
Received 12 December 2015
Received in revised form
18 May 2016
Accepted 31 May 2016
Available online 1 June 2016

Keywords:
Delamination
Composite beam
Vibration
Finite element method (FEM)

ABSTRACT

Delamination is a major damage mode in laminated composite structures which causes reduction in stiffness and strength and affects their vibration characteristics. This paper deals with the effects of delamination size and its thickness-wise and lengthwise location on the vibration characteristics of cross-ply laminated composite beams. Free and constrained mode models are introduced and compared in the analytical and finite element methods for the first three modes and a comprehensive discussion among these results is done. To verify the results, modal tests were carried out on the delaminated specimens. Unlike the available experimental research, the proportion of delamination size to the beam length (a/L) is relatively small (i.e., a/L=0.20, 0.10 and 0.05). Moreover, these experiments are focused on the effect of the axial location of delamination on the first three natural frequencies. All results are considered under both the clamped-free and clamped-clamped boundary conditions. Finally, some interesting relationships are presented between the frequencies reduction and their corresponding mode shapes, which can be useful for delamination detection.

1. Introduction

Composite materials are widely used in aeronautical, marine and automotive industries because of their excellent mechanical properties, low density, ease of manufacture and fatigue resistance. However, composites are very sensitive to the anomalies induced during their fabrication or service life. One of the commonly encountered types of defects or damage in laminated composite structures is delamination. Delaminations may originate during fabrication or may be service-induced, such as by impact or fatigue loading. Delaminations not only affect the strength of the structure, but also cause reduction in the stiffness, thus affecting its vibration and stability characteristics. Reflections of these effects in dynamic response are the alteration of natural frequencies and damping ratios. As a result, considerable analytical, numerical and experimental efforts have been conducted in the literature to study the damage evaluation (forward problem, i.e., to evaluate the effect of delamination on the vibration dynamic response, such as natural frequencies and mode shapes) and damage detection (inverse problem, i.e., to detect the location and size of delamination) of the delaminated composite structures.

One of the earliest models for vibration analysis of composite beams including delaminations was proposed by Ramkumar et al. [1]. They modeled a beam with one through-thickness delamination by simply using four Timoshenko beams connected at delamination edges. To study the influence of a through-thickness delamination on the free vibration of an isotropic beam, Wang et al. [2] presented an analytical model using four Euler–Bernoulli beams that are joined together. These two investigations assumed that the delaminated layers deform freely without touching each other ("free mode model").

Later, Mujumdar and Suryanarayan [3] presented two models namely the free mode model and the constrained mode model for the flexural vibrations of isotropic beams with delamination at the mid-plane as well as at the off-mid-plane locations. Experimental results have also been presented for various cases of delaminations in the beams. The "constrained model" fails to explain the delamination opening modes found in experiments [4–6].

An analytical model based on the Timoshenko beam theory is presented by Hu and Hwu [7] for the free vibrations of delaminated sandwich beams. Lee [8] presented a displacement-based layer-wise finite element model for the analysis of free vibration of delaminated beam. The effects of the fiber angle, location, size and numbers of delaminations are investigated numerically. A review paper on the vibration-based model-dependent damage (delamination) identification and health monitoring for composite structures is presented by Zou et al. [9]. This paper deals with various

* Corresponding author.
E-mail address: kvntrb@kashanu.ac.ir (K. Torabi).

http://dx.doi.org/10.1016/j.ijmecsci.2016.05.023
0020-7403/

models proposed for the free vibrations of delaminated beams. In the analytical research done by Luo and Hanagud [10], a piecewise-linear spring model is used to simulate the behavior among delaminated surfaces. Shear and rotary inertia effects, as well as bending-extension coupling, are included in the governing equations. Karmakar et al. [11] presented the effect of delamination on free vibration characteristics of graphite–epoxy composite pretwisted shallow shells of various stacking sequences considering length of delamination as a parameter. Perel [12] developed a new approach is for the dynamic analysis of a composite beam with an interply crack, in which a physically impossible interpenetration of the crack faces is prevented by imposing a special constraint, leading to taking account of a force of contact interaction of the crack faces and to nonlinearity of the formulated boundary value problem. The model is based on the first-order shear deformation theory and the shear deformation and rotary inertia terms are included into the formulation, to achieve better accuracy. Linear eigenvalue analysis showed decrease of natural frequencies upon increase of the crack length, and crack opening and closing during the vibration in higher mode shapes, beginning from the fifth one.

An exhaustive review on the vibration of delaminated composites has been presented by Della et al. [13]. They developed analytical solutions to study the free vibrations of multiple delaminated beams under axial compressive loadings [14]. Ramtekkar [15] presented free vibration analysis of laminated beams with delamination using mixed finite element model. Analytical solutions for beams with multiple delaminations have been presented by some researchers. Shu and Della [16,17] and Della and Shu [18] used the free mode and constrained mode assumptions to study a composite beam with various multiple delamination configurations. Their study emphasized the influence of a second delamination on the first and second natural frequencies and the corresponding mode shapes of a delaminated beam.

An improved dynamic analysis of delaminated bi-layer beams presented by Qiao and Chen [19] with considerations of transverse shear and delamination tip deformations as well as effects of friction and contact ahead of the delaminated tips. Manoach et al. [20] presented dynamic behavior of a composite beam having delamination and took into account a contact interaction among sublaminates including normal forces, shear forces and additional damping. Numerical calculations are performed in order to estimate the influence of the new terms included in the model. Muc and Stawiarski [21] introduced and used effective theoretical and computational (the finite element method) procedures to characterize the dynamic behavior of beams and of cylindrical panels with circular cross-section.

Two review papers on the vibration analysis and damage detection of composite structures are presented by Senthil et al. [22] and Thombare et al. [23]. The principal aim of the first paper [22] is to present a comprehensive literature survey on the defects, like debonds/delamination in composite joints/structures, focusing on the effect of defects, its growth initiation and prediction methods in fiber reinforced plastics. The other review study [23] focused on the damage detection in composite structures due to delamination with the help of vibration parameters. Additionally, some of case studies were also analyzed by the recent literatures. It has been observed that vibration technique is an effective method to detect delamination in composite structures. A new method of modeling partial delamination in composite beams is proposed and implemented by Kumar et al. [24] using the finite element method. Liu and Shu [25] developed analytical solutions to study the free vibrations of rotating Timoshenko beams with multiple delaminations.

Kargarnovin et al. [26] presented a rather new semi-analytical method towards investigating the free vibration analysis of generally laminated composite beam (LCB) with a delamination. At first, the combined effects of material couplings (bending–tension, bending–twist, and tension–twist couplings) with the effects of shear deformation, rotary inertia and Poisson's effect are taken into account. Then, the semi-analytical solution for the natural frequencies and mode shapes are presented by incorporating the constraint conditions using the method of Lagrange multipliers. Kargarnovin et al. [27] also modeled a composite beam with single delamination traveled by a constant amplitude moving force accounting for the Poisson's effect, shear deformation and rotary inertia. Shariati-Nia et al. [28] presented an analytical method for calculation of natural frequencies of a delaminated composite beam from both free and constrained mode frequencies. An improved combined natural frequency is proposed in this new formulation based on the breathing of delamination.

Szekrenyes [29] developed a novel analytical model to solve the problem of free vibration of delaminated composite beams. The most important aspect of this analysis is that the beams of the delaminated region are subjected to normal forces, as well. That is the essential reason for leading to a coupled flexural–longitudinal vibration problem. Moreover, it was shown that the delaminated beam vibration is a coupled flexural–longitudinal vibration using the simple and Timoshenko beam theories and there is parametric excitation in the delaminated part of the beam. Szekrenyes [30] also has presented the problem of free vibration of delaminated composite beams by showing the existence of parametric excitation, bifurcation and stability. Moreover, the parametric excitation of the delaminated part and the dynamic stability aspect of the problem was investigated and solved in this paper. Furthermore, the free vibration mode shapes in the state of instability are predicted based on the critical dynamic force and the condition of constant arc length of the delaminated parts.

Furthermore, considerable investigations have been conducted to study the damage detection (inverse problem) of the delaminated composite structures [31–34]. Zhang et.al [31] examined three different inverse algorithms for solving the non-linear equations to predict the interface, location and size of delamination: direct solution using a graphical method, artificial neural network (ANN) and surrogate-based optimization. Thalapil and Maiti [34] developed an analytical method to address both forward problem natural frequencies determination knowing the beam and crack geometry details as well as inverse problem of detection of crack with the knowledge of changes in the beam natural frequencies. They examined both long (Euler–Bernoulli) and short (Timoshenko) beams numerically.

This paper is an attempt to analyze the natural vibration of monolithic beams with longitudinal cracks for developing a method for its detection.

In this research, the analytical solution for the vibration of delaminated composite beams is formulated based on the free and constrained mode models. A finite element model is developed based on the assumptions of these two analytical models to calculate the natural frequencies and mode shapes. To assess the theoretical results, modal tests were carried out on delaminated composite specimens. Finally, an approach is developed by comparing the first several natural frequencies of specimens with the different delamination sizes and axial locations and mode shapes of intact specimens.

2. Problem statement

Fig. 1 shows a beam with a single delamination at an arbitrary location and various lengths which is modeled as four interconnected beams. L, h and a are beam length, beam thickness and delamination length, respectively.

The beam is separated along the interface by a delamination

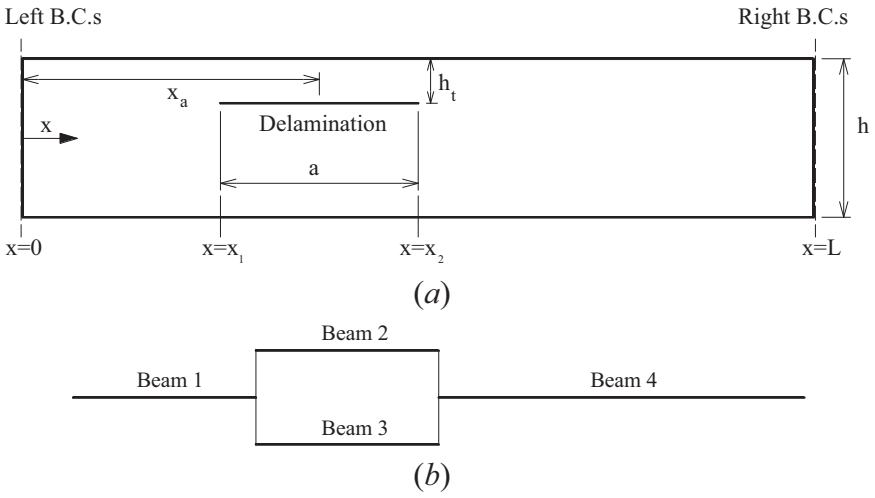

Fig. 1. a) Geometry of the delaminated beam, b) model of delaminated beam with four interconnected beams.

with length a which is located at arbitrary location through thickness and along the length of the beam. This beam can be subdivided into three span-wise regions, a delamination region and two integral regions. The delamination region is comprised of two segments (delaminated layers), beams 2 and 3, which are joined at their ends to the integral segments, beams 1 and 4. Each of the four beams is treated as beams with different boundary conditions.

Numerical investigations are undertaken for the free vibrations of cross-ply laminated beams with embedded internal delaminations of different sizes and at several different locations. For this purpose, an eight-layer symmetric cross-ply laminated $[0/90]_{2s}$ beam, under the clamped-free (CF) and clamped-clamped (CC) supports is considered. Thickness direction delamination locations are defined as mentioned in Fig. 2 "Interface 1" implies the mid-plane delamination, while "Interface 4" implies the skin ply delamination and so on. Furthermore, lengthwise delamination locations are various on the beam length. Fig. 2 shows interfaces and dimensions for a cross-ply delaminated beam schematically.

3. Analytical modeling of a delaminated composite beam

In this section, an analytical solution for the vibration of delaminated composite beams is formulated. Based on the assumptions in vibration of delaminated layers and complicate contact conditions, two approaches are used in analytical modeling, free and constrained mode models. The first model assumes that the delaminated layers deform freely without touching each other, and the second one proposes a constrained mode where the delaminated layers are assumed to be in touch along their whole length all the time, but are allowed to slide over each other. In fact, a delamination may breathe (open and close) during the vibration and the assumptions of the free or constrained mode models are not completely correct in the whole of the vibration period. For this reason, the combined vibration modes were presented by some researchers [28,30]. Furthermore, a constrained mode model can be obtained by utilizing a free mode model by artificially changing the densities in the top and bottom beams of the delaminated part and taking the conservation law of mass into consideration [29,30].

3.1. Free mode model

In free mode model, it is assumed that the delaminated layers deform freely without touching each other and have different transverse deformations. Since the beam is comparatively thin (h/b is less than 10 and h/L is less than 100), the governing equations for the free vibration of a delaminated beam using the Euler–Bernoulli beam theory are

$$D_i\frac{\partial^4 w_i}{\partial x^4}+m_i\frac{\partial^2 w_i}{\partial t^2}=0 \quad i=1, 2, 3, 4 \tag{1}$$

where D_i is the equivalent bending stiffness of the ith beam, m_i is the mass per unit length and is equal to $\rho_i A_i$, ρ_i is the mass density and A_i is the cross-sectional area of the beam. The bending stiffness for homogeneous and isotropic beams is given by $D_i=EI_i$, where E denote the Young's modulus and I is the moment of inertia. The mechanical properties of the composite beams are determined using the classical lamination theory (CLT) as

$$D_i=D_{11}^{(i)}-\frac{\left(B_{11}^{(i)}\right)^2}{A_{11}^{(i)}} \tag{2}$$

where $A_{11}^{(i)}$ is the extensional stiffness, $B_{11}^{(i)}$ is the bending–extension coupling stiffness, $D_{11}^{(i)}$ is the bending stiffness of the ith

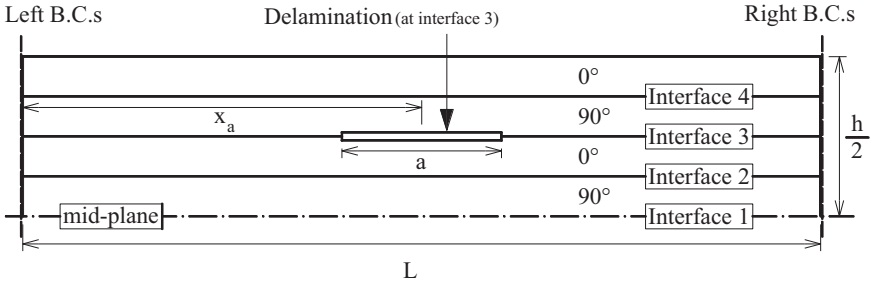

Fig. 2. Geometry of the eight layer symmetric composite laminated beam $[0/90]_{2s}$ (various interfaces for delamination).

beam [7].

For free vibration, the solution of Eq. (1) is given as

$$w_i(x, t)=W_i(x)e^{j\omega t} \tag{3}$$

where ω is the natural frequency and W_i is the mode shape. Substituting Eq. (3) into Eq. (1) and eliminating the trivial solution $\sin(\omega t)=0$, one can obtain the general solutions of the differential equation in Eq. (1) as

$$W_i(x)=C_i\ \cos(\lambda_i x)+S_i\ \sin(\lambda_i x)+CH_i\ \cos h(\lambda_i x)+SH_i \sin h(\lambda_i x) \tag{4}$$

where

$$\lambda_i{}^4=\frac{m_i\omega^2}{D_i} \tag{5}$$

and λ_i are the non-dimensional frequencies. The lowest eigenvalue λ is the non-dimensional primary frequency of the beam. The 16 unknown coefficients C_i, S_i, CH_i and SH_i are determined by four boundary conditions and twelve continuity conditions.

For cantilever beams, boundary conditions at fixed end ($x=0$) are $W_1=0$, $W_1'=0$ and at free end ($x=L$) are $W_4''=0$, $W_4'''=0$. Similarly, four boundary conditions at two ends of beam with CC and simply supports are respectively $W_1=0$, $W_1'=0$, $W_4=0$, $W_4'=0$ and $W_1=0$, $W_1''=0$, $W_4=0$, $W_4''=0$.

Also, continuity conditions at $x=x_1$ are [3,17]

$$W_1=W_2,\ W_1=W_3 \tag{6-1}$$

$$W_1'=W_2',\ W_1'=W_3' \tag{6-2}$$

$$D_1W_1'''=D_2W_2'''+D_3W_3''' \tag{6-3}$$

$$D_1W_1''+\beta\left[W_1'(x_1)-W_2'(x_2)\right]=D_2W_2''+D_3W_3'' \tag{6-4}$$

where

$$\beta=\frac{h^2}{4a}\left[\frac{A_{11}{}^{(2)}A_{11}{}^{(3)}}{A_{11}{}^{(2)}+A_{11}{}^{(3)}}\right] \tag{7}$$

The second term on the left side of Eq. (6-4) represents the contribution to the bending moment from the difference of stretching between beams 2 and 3 and contributes to the bending stiffness of the beam [3,16–18]. Similarly, the continuity conditions at the end tip of delamination ($x=x_2$) can be derived. The boundary conditions and continuity conditions provide 16 homogeneous equations for 16 unknown coefficients. A non-trivial solution for the coefficients exists only when the determinant of the coefficient matrix vanishes. The frequencies and mode shapes can be obtained as eigenvalues and eigenvectors, respectively.

3.2. Constrained mode model

The constrained mode model is simplified by the assumption that the delaminated layers are in touch along their whole length all the time, but are allowed to slide over each other. Therefore, the delaminated layers have the same transverse deformations ($w_3=w_2$). This is reasonable since if there is no opening in the delamination region, the free model and constrained model are essentially the same. In this model the governing equations for beam 1 and 4 are

$$D_i\frac{\partial^4 w_i}{\partial x^4}+m_i\frac{\partial^2 w_i}{\partial t^2}=0 \qquad i=1,4 \tag{8-1}$$

For beams 2 and 3

$$D_{23}\frac{\partial^4 w_2}{\partial x^4}+m_{23}\frac{\partial^2 w_2}{\partial t^2}=0 \tag{8-2}$$

where, $D_{23}=D_2+D_3$ and $m_{23}=m_2+m_3$.

The generalized solutions for the constrained model are identical in form to the free model. The unknown coefficients C_i, S_i, CH_i and SH_i, however, are reduced to twelve coefficients which can be determined by four boundary conditions and eight continuity conditions.

In this model, boundary conditions at two ends of the beam are the same as free mode model, but four continuity conditions at $x=x_1$ are [3,17]

$$W_1=W_2 \tag{9-1}$$

$$W_1'=W_2' \tag{9-2}$$

$$W_1'''=W_2''' \tag{9-3}$$

$$D_1W_1''+\beta\left[W_1'(x_1)-W_2'(x_2)\right]=D_{23}W_2'' \tag{9-4}$$

Similarly, four continuity conditions at the end tip of delamination ($x=x_2$) can be derived. These boundary and continuity conditions provide 12 homogeneous equations for 12 unknown coefficients.

4. Finite element modeling

The finite element modeling (FEM) for simulation of the delaminated beams and extraction of the natural frequencies and mode shapes was conducted using the commercial finite element software ABAQUS. As shown in Fig. 1, a delaminated beam is subdivided into four beams which are modeled separately by using the conventional shell elements. The composite laminates are meshed with S4R element available in the ABAQUS library. This element has linear geometric order, and has used a 4-node doubly curved thin or thick shell, reduced integration, hourglass control, finite membrane strains. A lamina elastic type is used for materials and composite continuum shell with Simpson's rule for thickness integration for sections definition. An eight-layer symmetric cross-ply laminated $[0/90]_{2s}$ beam is created and assigned as a section to the beams 1 and 4 (integral regions). According to interface of delamination, two different sections are created and assigned to the beams 2 and 3 (delamination region). Then these four beams are assembled and for modal analysis, a new step is created under procedure type: linear perturbation, Frequency.

Suitable constraints and interactions are defined in the assembled beams. At the delamination tips, three beams are attached to each other with “tie” constraint type which satisfies all continuity conditions. For the constrained mode model, a standard surface-to-surface contact interaction with tangential behavior property is introduced between the two faces of the delamination, which allowed neither penetration nor separation among the sublaminate structures. Therefore, the delaminated layers have the same transverse deformations and can slide over each other. For the free mode model, no interaction is defined between the surfaces of the delamination. Consequently, the elements on either side of the delamination deform freely and can separate and penetrate to each other effectively, causing a lower stiffness. The CF and CC boundary conditions are considered with fixing the clamped sides of assembled beams and definition and assignment of meshes are done. The numbers of nodes, elements and the degrees of freedom (DOFs) used in the model depend on the delamination length. For example, the total numbers of elements are 300 when dimensionless length of delamination (a/L) is 0.2, and DOF of each element is six.

5. Experimental investigation

To verify the analytical and finite element methods, modal tests were carried out on some specimens. The purpose of these experiments is to investigate the effects of delamination size and location on natural frequencies. In the experimental procedure delamination size is relatively small (dimensionless length, a/L is 0.20, 0.10 and 0.05) with respect to the available works in the literature and the location of delamination varies along the beam length.

5.1. Specimens preparation

Fourteen laminated composite beams were manufactured by hand layup method using glass/epoxy prepreg. The mechanical properties of unidirectional composite are measured according to the ASTM D3039 [35] for the longitudinal and transverse moduli as well as the Poisson's ratio. The in-plane shear modulus is measured using ASTM D3518 [36]. The stacking sequence of composite beams is $[0/90]_{2s}$. Specimens are cured inside the autoclave for one hour at 121 °C temperature and 3.45 bar pressure. The mechanical properties of unidirectional composite ply are presented in Table 1.

Delaminated specimens were cut and sized to width (b) 20 mm and length (L) 250 and 300 mm for cantilever and clamped-clamped beams, respectively. Total thickness (h) of all specimens is 1.2 mm. Delamination is artificially created by inserting a release film with thickness of 20 μm at the mid-plane (interface 1) of each laminate during the manufacturing. Two specimens as intact specimens were fabricated with no delamination.

5.2. Testing procedure and equipment

The test was carried out in the frequency range of 0–800 Hz. A B&K 8202 hammer with rubber and metal tip was used to excite the specimens and acceleration response was measured by a PCB 356A01 accelerometer in vertical direction. The FFT analyzer used to carry out and process the frequency response functions B&K Portable PULSE 3560D. Fig. 3 shows the experimental set up. A fixture is designed and manufactured for simulating the CF and CC boundary conditions. Total length of specimens is 250 mm for CF and 300 mm for CC. In fact, 50 mm of composite beams is used for clamped boundary condition. One specimen was tested three times and the average natural frequencies were reported. The standard deviation of experimental frequencies for first, second and third mode was less than 3, 1 and 0.25 Hz, respectively.

6. Results and discussions

6.1. Effect of thickness-wise location and long size of delamination on the natural frequencies

The fundamental frequencies of a delaminated composite beam with various sizes and locations through thickness for delamination and CF boundary conditions are presented in Tables 2–5. Delaminations are located at the center along the length of the beam with various thickness-wise locations and dimensionless length (a/L) of 0.2, 0.4, 0.6, and 0.8. In these tables, the results are presented for both constrained and free mode models from analytical and finite element methods. Also, the experimental and analytical results related to model A (constrained model) and model B (free model) are provided from Ref. [4] to assess the obtained results. Analytical model in this reference is based on the cracked beam theories [5,6] derived using Timoshenko beam theory and general kinematic assumptions.

Table 1
Mechanical properties of the laminated beam.

E_{11} (GPa)	E_{22} (GPa)	G_{12} (GPa)	υ_{12}	ρ (kg/m^3)
44.7	13.2	5.0	0.3	1942.5

The composite beam was modeled with length (L) 127 mm, width (b) 12.7 mm and total thickness (h) 1.016 mm. The material properties are: $E_{11}=134.49$ GPa, $E_{22}=10.34$ GPa, $G_{12}=5$ GPa, $\upsilon_{12}=0.33$ and density $\rho=1500$ kg/m^3. It is observed that the fundamental frequencies obtained from analytical and finite element method closely match with the experimental results of Ref. [4] for most of the cases.

In both analytical and finite element frequencies, by comparing constrained and free mode models, the natural frequencies obtained from free mode model were comparatively lower than the results of constrained mode model. This discrepancy can be attributed to the effect of contact among the delaminated surfaces during vibrations. The amount of this discrepancy increases for larger delamination length and finite element results are greater than analytical one.

In analytical results, there is no considerable difference between frequencies obtained from both constrained and free mode model at the first natural frequency. In finite element results, natural frequencies obtained from constrained mode have better agreement with those from free mode for all cases. Also, when delamination length increases or delamination is moved from the surface to the mid-plane of the beam, constrained mode frequencies matched better with experimental frequencies.

Tables 6 and 7 show the second and third natural frequencies for delamination along interface 3. The results are obtained from the analytical and finite element methods for constrained and free mode models. Also, the second natural frequencies are presented from Ref. [15] for comparison in Table 6. These analytical results are obtained using mixed finite element model and presented for both constrained mode model (contact-interface model) and free mode model (unconstrained-interface model).

In both analytical and finite element results, the difference between the frequencies of constrained and free mode models increases at the higher modes. All natural frequencies obtained from the constrained mode have better agreement with those from free mode for all cases. By comparing the first three mode shapes of the cantilever beam, it can be concluded that for each mode, this discrepancy decreases when the delamination is located on the nodes of that mode shape.

In analytical results, there is no considerable difference between constrained and free mode frequencies for small delamination lengths ($a/L<0.3$), especially in lower modes. The second and third analytical frequencies in Tables 6 and 7 are significantly distinguished between the free and constrained models and differ greatly for larger amount of ratios a/L. It's reasonable at the higher modes and for larger delamination length, by increasing the delamination breathing, the difference between these two models increases.

Figs. 4 and 5 show the first three mode shapes for constrained and free mode models from finite element analysis respectively. Delamination dimensionless length (a/L) is 0.4 and located along the interface 4. Elements with blue color show points with no deflection and refer to nodes of mode shapes.

6.2. Effect of lengthwise location and small size of delamination on the natural frequencies

In the available experimental tests in the literature, such as those used in the previous section, the effect of delamination

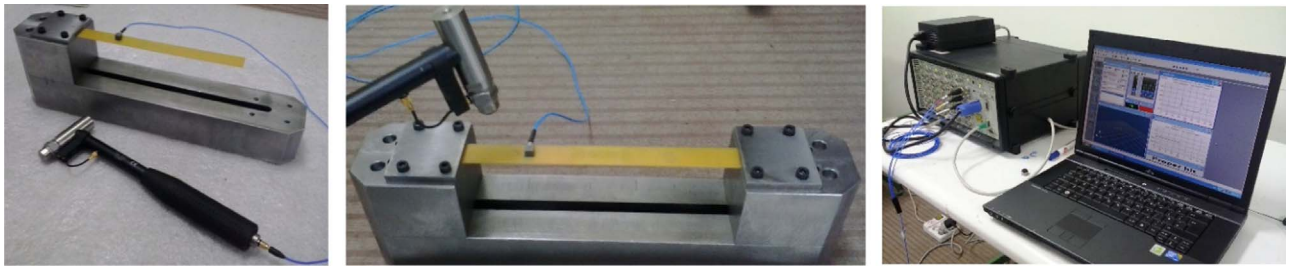

Fig. 3. Experimental test setup for CF and CC boundary conditions.

Table 2
Fundamental natural frequency (Hz) for delamination along interface 1.

$\frac{a}{L}$	Shen and Grady [4]			Present study			
	Exp.	Theory		FEM		Theory	
		Const.	Free	Const.	Free	Const.	Free
0.0	79.83	82.04	82.04	82.12	82.12	82.21	82.21
0.2	78.17	80.13	67.36	80.17	68.67	80.41	80.41
0.4	75.37	75.29	56.48	75.60	58.09	75.27	75.27
0.6	67.96	66.94	47.90	66.64	48.97	66.40	66.40
0.8	57.54	57.24	40.59	56.18	41.16	56.29	56.29

Table 3
Fundamental natural frequency (Hz) for delamination along interface 2.

$\frac{a}{L}$	Shen and Grady [4]			Present study			
	Exp.	Theory		FEM		Theory	
		Const.	Free	Const.	Free	Const.	Free
0.0	79.83	82.04	82.04	82.12	82.12	82.21	82.21
0.2	77.79	81.39	68.78	79.80	67.72	80.56	80.56
0.4	75.13	78.10	59.44	75.56	57.02	75.87	75.87
0.6	66.96	71.16	51.18	67.13	48.12	67.60	67.60
0.8	48.34	62.12	43.86	57.06	40.59	57.89	57.89

Table 4
Fundamental natural frequency (Hz) for delamination along interface 3.

$\frac{a}{L}$	Shen and Grady [4]			Present study			
	Exp.	Theory		FEM		Theory	
		Const.	Free	Const.	Free	Const.	Free
0.0	79.83	82.04	82.04	82.12	82.12	82.21	82.21
0.2	80.13	81.46	75.14	81.00	78.32	81.61	81.61
0.4	79.75	79.93	70.42	79.70	73.96	80.00	79.97
0.6	76.96	76.71	65.06	76.69	68.58	76.77	76.56
0.8	72.46	71.66	59.13	72.00	62.10	71.99	71.04

Table 5
Fundamental natural frequency (Hz) for delamination along interface 4.

$\frac{a}{L}$	Shen and Grady [4]			Present study			
	Exp.	Theory		FEM		Theory	
		Const.	Free	Const.	Free	Const.	Free
0.0	79.83	82.04	82.04	82.12	82.12	82.21	82.21
0.2	79.96	81.60	75.83	80.88	79.75	81.70	81.70
0.4	68.92	80.38	71.88	79.70	76.63	80.34	80.32
0.6	62.50	77.70	67.18	76.96	72.28	77.60	77.46
0.8	55.63	73.15	61.70	72.66	66.64	73.44	72.75

Table 6
Second natural frequency (Hz) for delamination along interface 3.

$\frac{a}{L}$	Ramtekkar [14]		Present study			
	Theory		FEM		Theory	
	Const.	Free	Const.	Free	Const.	Free
0.0	519.24	519.24	514.02	514.02	515.26	515.26
0.2	514.13	513.23	493.59	441.50	504.13	503.20
0.4	508.61	440.30	497.61	378.81	493.25	443.45
0.6	486.75	226.02	483.71	451.89	470.99	238.39
0.8	436.96	128.56	438.10	423.84	427.71	139.18

Table 7
Third natural frequency (Hz) for delamination along interface 3.

$\frac{a}{L}$	FEM		Theory	
	Const.	Free	Const.	Free
0.0	1437.00	1437.00	1442.89	1442.89
0.2	1374.50	1372.40	1382.04	1381.59
0.4	1172.10	1102.00	1186.15	644.11
0.6	1156.40	1064.00	1076.74	525.88
0.8	1060.30	1043.10	1055.06	369.50

dimensionless lengths (a/L) are presented only for the large sizes of delaminations (i.e., $a/L > 0.2$) and only the first natural frequencies are measured. Here, it is focused on the small sizes of delamination (i.e., $a/L = 0.05$ to 0.2), and the first three natural frequencies are measured. Furthermore, the effect of delamination location along the beam length is investigated for both CC and CF boundary conditions. The composite beam was simulated with length (L) 200 mm, width (b) 20 mm and total thickness (h) 1.2 mm. Material properties of unidirectional composite ply are presented in Table 1.

The beams were tested and modeled in two boundary conditions: CC as symmetric boundary conditions and CF as unsymmetric boundary conditions. The results of previous section on the effect of delamination location through thickness on the natural frequencies show that the constrained mode model have good agreement with experiments compared to the free mode model. Therefore, only results of this model are presented for analytical and finite element methods in this section. Also, results of natural frequencies are presented for single delamination located at various lengthwise locations. Tables 8–10 show the first three natural frequencies for beams with CF and CC boundary conditions. Delamination lengths (a/L) is 0.2 and are located in interface 1 (midplane) through the thickness for all cases. Delamination location along the length of the beam (x_a/L) is 0.15, 0.50, and 0.85 for CF boundary conditions. Because of geometrical symmetry in CC boundary conditions, delamination location (x_a/L) is 0.15, 0.30, and 0.50.

It is seen that delaminations with equal lengths, same thickness-wise locations and various lengthwise locations have

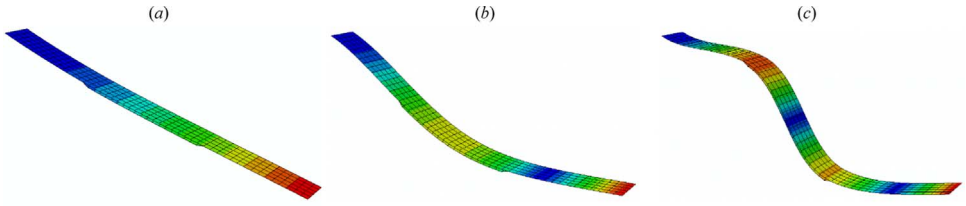

Fig. 4. First three mode shapes of delaminated cantilever beam (Interface 4 and $a/L=0.4$) for constrained mode model a) 1st mode, b) 2nd mode, c) 3rd mode. (For interpretation of the references to color in this figure, the reader is referred to the web version of this article.)

different effects on the first three natural frequencies.

The first three natural frequencies of composite beams with different sizes of delamination along the interface 1 (mid-plane) are presented in Tables 11–13. Delaminations are located at the center along the length of the beam with dimensionless length (a/L) of 0.05, 0.10, and 0.20. When $a/L=0$, it shows the intact or healthy state for the beam.

These results show that delaminations with small length ($a/L<0.2$) don't have considerable effect on natural frequencies especially in lower modes.

Results in Tables 8–13 show that the finite element results based on constrained mode model are in good agreement with analytical results, but they overestimate the experimental results. The difference between theoretical results and experiment is about 5%, 11%, 17% for CF and 9%, 15%, 14% for CC in the first, second and third modes, respectively. This difference may be due to the effect of the accelerometer sensor attached on the specimens, which acts as a concentrated mass (1 g) [37]. Since the location of the sensor, as a concentrated mass, is the same in all specimens (at the point of a quarter of the length), the value of frequency reduction in the intact and delaminated beams are equal and has no influence on measured frequency reduction in delaminated specimen rather than intact one. Also, other sources of differences between the results arise from the experimental equipment and preparation of specimens.

6.3. Frequencies reduction and its relationship with mode shapes

Here, we try to show the effect of delamination size and axial location on the first several natural frequencies of the above described composite beam. Also, these effects are compared with related mode shapes and a new procedure is obtained that will be useful for delamination detection especially its axial location. Both CC and CF as symmetric and unsymmetric boundary conditions are considered. The percentage of frequency reduction (normalized frequency) due to the delamination in each mode is a function of the delamination size and location and introduced as follows:

$$\Delta\omega = \frac{\omega_u-\omega_d}{\omega_u}*100 \tag{10}$$

where ω_u and ω_d are respectively the frequencies of the undelaminated and the delaminated beams in each mode.

Figs. 6 and 7 present the effect of delamination axial location on the first three natural frequencies for CC and CF boundary conditions, respectively. For each mode, the calculated frequency has been normalized to the frequencies of undelaminated cases. These analytical results for the first three modes are shown with solid line, dashed line and dotted line respectively. For this analysis, a mid-plane delamination (interface 1) with $a/L=0.20$ is

Table 8
First constrained mode natural frequency (Hz).
For CF and CC boundary conditions (with various locations of delamination).

CF				CC			
$\frac{x_a}{L}$	Exp.	Theory	FEM	$\frac{x_a}{L}$	Exp.	Theory	FEM
Intact	19.75	20.87	20.63	Intact	120.80	132.78	131.30
0.15	19.00	19.77	19.94	0.15	111.60	120.44	118.77
0.50	19.50	20.54	20.38	0.30	115.00	125.89	124.52
0.85	19.70	20.84	20.58	0.50	118.50	129.55	129.39

Table 9
Second constrained mode natural frequency (Hz).
For CF and CC boundary conditions (with various locations of delamination).

CF				CC			
$\frac{x_a}{L}$	Exp.	Theory	FEM	$\frac{x_a}{L}$	Exp.	Theory	FEM
Intact	116.50	130.77	129.21	Intact	310.00	366.02	361.56
0.15	107.80	117.95	116.13	0.15	286.00	315.04	310.40
0.50	115.50	126.18	126.65	0.30	308.50	354.79	355.92
0.85	114.00	127.58	125.98	0.50	286.50	323.41	317.77

Table 10
Third constrained mode natural frequency (Hz).
For CF and CC boundary conditions (with various locations of delamination).

CF				CC			
$\frac{x_a}{L}$	Exp.	Theory	FEM	$\frac{x_a}{L}$	Exp.	Theory	FEM
Intact	302.50	366.17	361.59	Intact	615.50	717.54	707.92
0.15	270.00	315.44	310.50	0.15	584.00	641.18	636.23
0.50	273.50	320.75	314.81	0.30	578.00	610.37	600.59
0.85	288.30	340.06	336.71	0.50	598.50	686.59	689.58

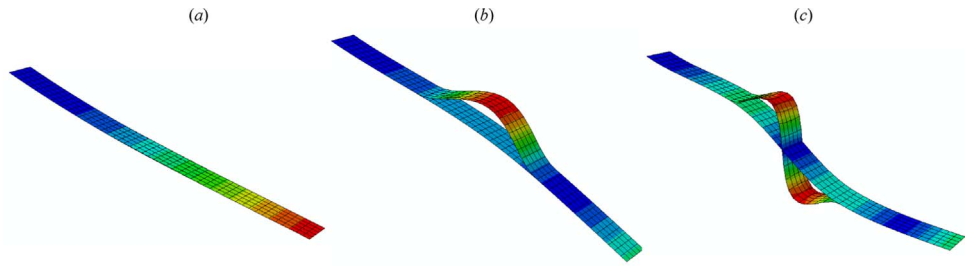

Fig. 5. First three mode shapes of delaminated cantilever beam (Interface 4 and $a/L=0.4$) for free mode model a) 1st mode, b) 2nd mode, c) 3rd mode. (For interpretation of the references to color in this figure, the reader is referred to the web version of this article.)

Table 11
First constrained mode natural frequency (Hz).
For CF and CC boundary conditions (with various size of delamination).

$\frac{a}{L}$	CF			CC		
	Exp.	Theory	FEM	Exp.	Theory	FEM
0.00	19.75	20.87	20.63	120.80	132.78	131.30
0.05	19.75	20.82	20.53	121.00	131.89	129.71
0.10	19.75	20.76	20.51	120.50	131.05	129.48
0.20	19.50	20.54	20.38	118.50	129.55	129.39

Table 12
Second constrained mode natural frequency (Hz).
For CF and CC boundary conditions (with various size of delamination).

$\frac{a}{L}$	CF			CC		
	Exp.	Theory	FEM	Exp.	Theory	FEM
0.00	116.50	130.77	129.21	310.00	366.02	361.56
0.05	116.30	129.55	126.85	309.40	365.15	360.66
0.10	116.30	128.39	126.73	309.50	359.32	354.61
0.20	115.50	126.18	126.65	286.50	323.41	317.77

Table 13
Third constrained mode natural frequency (Hz).
For CF and CC boundary conditions (with various size of delamination).

$\frac{a}{L}$	CF			CC		
	Exp.	Theory	FEM	Exp.	Theory	FEM
0.00	302.50	366.17	361.59	615.50	717.54	707.92
0.05	301.50	365.24	360.43	611.50	711.11	697.06
0.10	298.00	359.06	354.03	611.50	705.48	695.16
0.20	273.50	320.75	314.81	598.50	686.59	689.58

moved along the beam length. Axial position of delamination (x_a/L) is varied from 0.1 to 0.9. Also, the related mode shapes for each mode numbers are presented.

It is obvious from Figs. 6 and 7 that the first mode has the minimum frequency changes and higher modes have higher changes. The effect of the axial location of delamination on the frequency changes percentage is noticeable and varies up to 6 times. In other words, the axial location of delamination affects the certain frequencies up to 15%.

In both symmetric and unsymmetric boundary conditions (CC and CF) and in all three shown modes, when the axial position of delamination center is located on the node of a mode shape, the frequency changes of that mode increases. Conversely, the minimum changes of each frequency occur when axial locations of delamination are located on the antinodes of that mode. In other words, the local maximums of frequency change graphs are coincided with node points of mode shapes, and their local minimums coincided with antinode points of mode shapes. The effect of delamination on natural frequencies increases near the supports (clamped edges) due to boundary conditions. Since the support points are node points for all modes, frequency changes in these points are maximum in all graphs especially in lower modes.

Figs. 8 and 9 show the first four normalized frequencies of a beam with a mid-plane delamination centered at $x_a/L=0.5$ as a function of the normalized delamination length (a/L), respectively for CC and CF boundary conditions. These analytical results for the first four modes are shown with solid line, dashed line, dash–dot line and dotted line respectively.

At the shorter delamination length all four modes approach the values of an undelaminated beam. Also, it is obvious from these figures that the first mode has the minimum frequency changes. For example, in CC boundary condition with a delamination length of 40% ($a/L=0.4$) frequency reduction for the first mode is 6% while for higher modes are more than 25%. The largest delamination (whole of the specimen length) had no more than a 50% change on any of the frequencies measured.

Considering the axial location of delamination (located at the center of the beam), and by comparing frequency change graphs with related mode shapes, it is found that at the short delamination length ($a/L<0.3$), frequency changes in the modes whose delamination is located on its nodes is more than the modes

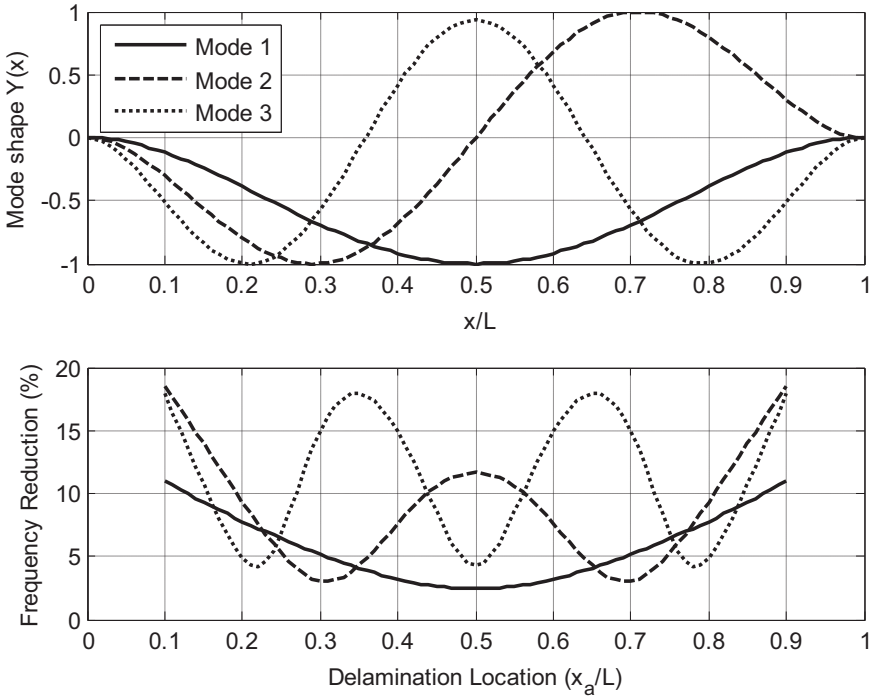

Fig. 6. Effect of delamination axial location on natural frequencies of a delaminated composite beam, For CC boundary condition with 20% delamination length ($a/L=0.20$).

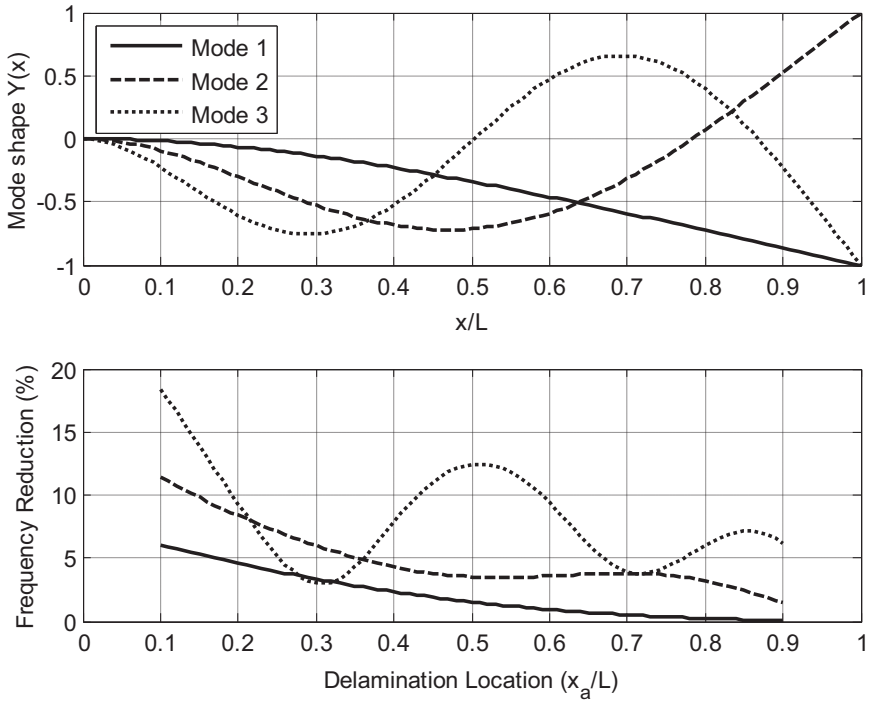

Fig. 7. Effect of delamination axial location on natural frequencies of a delaminated composite beam, For CF boundary condition with 20% delamination length ($a/L=0.20$).

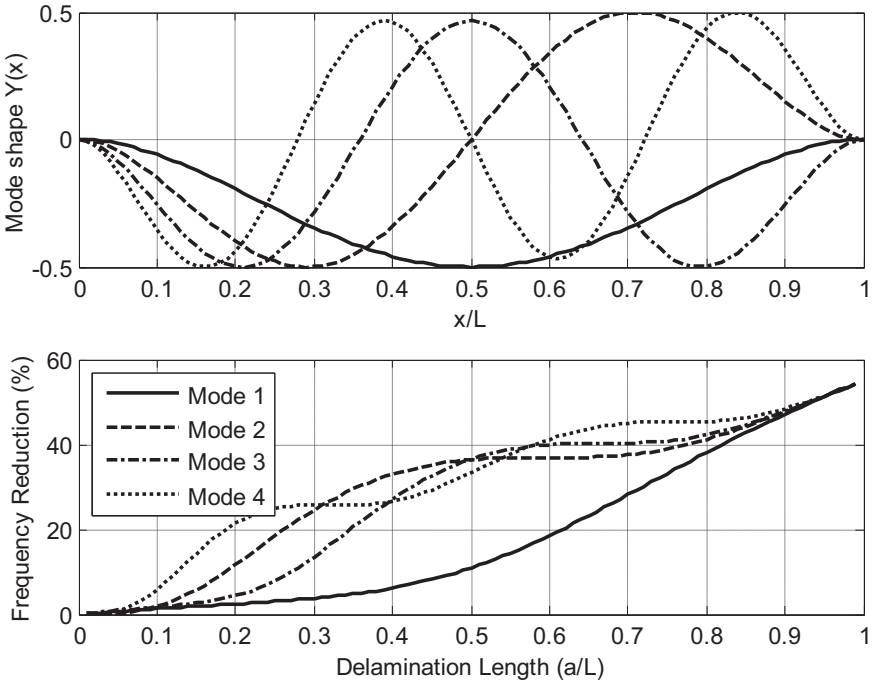

Fig. 8. Effect of delamination size on natural frequencies of a delaminated composite beam, For CC boundary conditions with a mid-plane delamination centered at $x_a/L=0.5$.

whose delamination is located on its antinodes. For example, in CC boundary condition, antinode and node of mode shape are located at the center of the beam respectively for odd and even modes. This is why, frequency changes in second and fourth modes are more noticeable than the first and third modes for $a/L<0.3$.

Increasing delamination length, when delamination tips meet antinodes of mode shapes, frequency changes decrease and graphs reach to horizon. On the other hand, when delamination tips cross the nodes of mode shapes, frequency changes increases and graphs get higher slopes. For a/L between 0.5 and 0.7 in the second mode of CC boundary condition, the delamination does not reduce the frequency anymore since it is moving into a region of antinodes. The same results in CF boundary condition are also as unsymmetric boundary conditions.

7. Conclusions

A comparative study is performed among the analytical, finite element and experimental results of the vibration characteristics of a delaminated cross-ply composite beam with various boundary conditions. Two models, i.e., free and constrained mode models

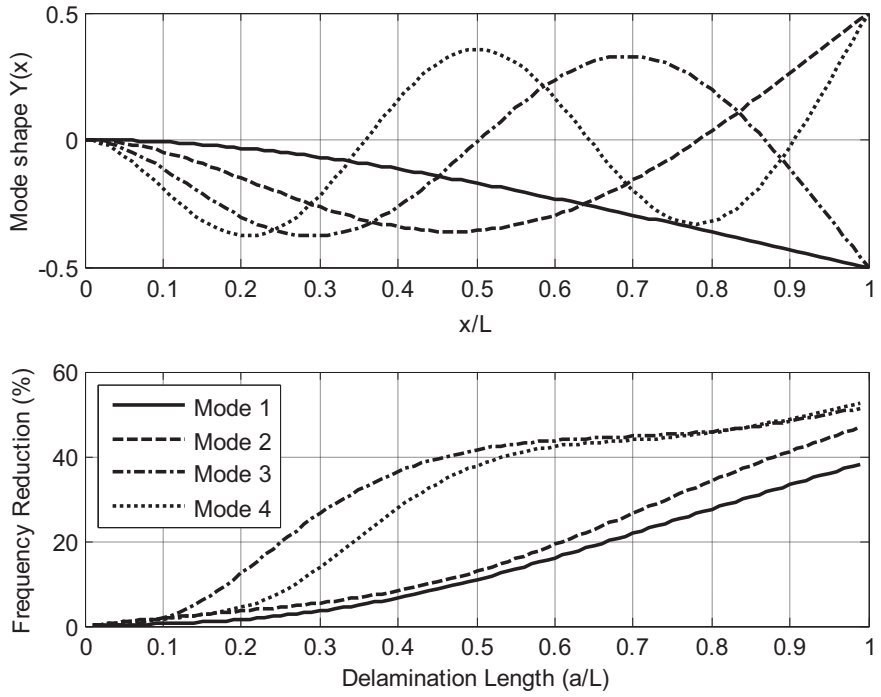

Fig. 9. Effect of delamination size on natural frequencies of a delaminated composite beam, For CF boundary conditions with a mid-plane delamination centered at $x_a/L=0.5$.

are taken into account in the analytical and finite element modeling. The experiments have been focused on the effect of small delamination length (dimensionless length, a/L is 0.20, 0.10 and 0.05) and its axial location on the first three natural frequencies. It is observed that the frequencies obtained from the analytical and finite element methods are closely matched with each other and have good agreement with the experimental results for most of the cases. The numerical results show delamination change the natural frequencies of a composite beam and the amount of reduction depends not only on the size of delamination but also on its location through-the-thickness and the length of the beam.

In both analytical and finite element frequencies, by comparing constrained and free mode models, the natural frequencies obtained from free mode model were comparatively lower than the results of constrained mode model. This difference increases at the higher modes and for larger delamination length and in the finite element results, it is more than the analytical one. Also, the amount of this difference decreases when the delamination is located on the nodes of that mode shape. In analytical results, there is no considerable difference between frequencies obtained from both the constrained and free mode model for small delamination lengths, especially in lower modes, while all natural frequencies obtained from the constrained mode have better agreement with those from the free mode for all cases in finite element results, especially for larger delamination lengths.

In the next step, by using these results and the effect of lengthwise location and size of delamination on the natural frequencies, some interesting relationships were presented between the frequencies reduction and their corresponding mode shapes, which can be useful in delamination detection. The first mode has the lowest frequency changes and higher modes have maximum changes. In each mode, when the delamination is located in the regions of mode shape antinodes, low reduction is observed. Conversely, the maximum reduction in frequency was observed when delamination is located in the regions of mode shape nodes. The effect of delamination is reduced when the delamination is moved from the region of mode shape nodes to region of mode shape antinodes.

Acknowledgment

The authors are grateful to the University of Kashan for supporting this work by Grant No. 463872/1.

References

[1] R.L. Ramkumar, S.V. Kulkarni, R.B. Pipes. Free vibration frequencies of a delaminated beam. In: proceedings of the 34th annual technical conference of reinforced plastics/composites institute, Vol. 22. The Society of the Plastics Industry Inc.; 1979. p. 1–5.
[2] Wang JTS, Liu YY, Gibby JA. Vibration of split beams. J Sound Vib 1982;84(4):491–502.
[3] Mujumdar PM, Suryanarayan S. Flexural vibrations of beams with delaminations. J Sound Vib 1988;125(3):441–61.
[4] Shen MHH, Grady JE. Free vibrations of delaminated beams. AIAA J 1992;30(5):1361–70.
[5] Shen MHH, Pierre C. Natural modes of Bernoulli-Euler beams with symmetric cracks. J Sound Vib 1990;138(1):115–34.
[6] Shen MHH, Pierre C. Free vibrations of beams with a single-edge crack. J Sound Vib 1994;170(2):237–59.
[7] Hu JS, Hwu C. Free vibration of delaminated composite sandwich beams. AIAA J 1995;33(10):1911–8.
[8] Lee J. Free vibration analysis of delaminated composite beams. Comput Struct 2000;74:121–9.
[9] Zou Y, Tong L, Steven GP. Vibration-based model-dependent damage (delamination) identification and health monitoring for composite structures – A review. J Sound Vib 2000;230(2):357–78.
[10] Luo H, Hanagud S. Dynamics of delaminated beams. Int J Solids Struct 2000;37:1501–19.
[11] Karmakar A, Roy H, Kishimoto K. Free vibration analysis of delaminated composite pretwisted shells. Aircr Eng Aerosp Technol 2005;77(6):486–90.
[12] Perel VY. Finite element analysis of vibration of delaminated composite beam with an account of contact of the delamination crack faces, based on the first-order shear deformation theory. J Compos Mater 2005;39(20):1843–76.
[13] Della CN, Shu D. Vibration of delaminated composite laminates: a review. Appl Mech Rev 2007;60(1):1–20.
[14] Della CN, Shu D. Free vibration analysis of multiple delaminated beams under axial compressive load. J Reinf Plast Compos 2009;28(11):1365–81.
[15] Ramtekkar GS. Free vibration analysis of delaminated beams using mixed finite element model. J Sound Vib 2009;328:428–40.
[16] Shu D, Della CN. Vibrations of multiple delaminated beams. Compos Struct 2004;64(3–4):467–77.
[17] Shu D, Della CN. Free vibration analysis of composite beams with two non-overlapping delaminations. Int J Mech Sci 2004;46:509–26.
[18] Della CN, Shu D. Free vibration analysis of composite beams with overlapping

delaminations. Eur J Mech A/Solid 2005;24:491–503.
[19] Qiao P, Chen F. On the improved dynamic analysis of delaminated beams. J Sound Vib 2012;331:1143–63.
[20] Manoach E, Warminski J, Mitura A, Samborski S. Dynamics of a composite Timoshenko beam with delamination. Mech Res Commun 2012;46:47–53.
[21] Muc A, Stawiarski A. Identification of damages in composite multilayered cylindrical panels with delaminations. Compos Struct 2012;94:1871–9.
[22] Senthil K, Arockiarajan A, Palaninathan R, Santhosh B, Usha KM. Defects in composite structures: Its effects and prediction methods – A comprehensive review. Compos Struct 2013;106:139–49.
[23] Thombare S, Jamadar NI, Kivade SB. Damage identification in composite structures due to delamination by vibration characteristics – A review. Int J Eng Sci and Innov Technol (IJESIT) 2014;3(6):108–15.
[24] Kumar SK, Ganguli R, Harursampath D. Partial delamination modeling in composite beams using a finite element method. Finite Elem Anal Des 2013;76:1–12.
[25] Liu Y, Shu DW. Free vibration analysis of rotating Timoshenko beams with multiple delaminations. Compos Part B: Eng 2013;44:733–9.
[26] Kargarnovin MH, Ahmadian MT, Jafari-Talookolaei RA, Abedi M. Semi-analytical solution for the free vibration analysis of generally laminated composite Timoshenko beams with single delamination. Compos Part B: Eng 2013;45:587–600.
[27] Kargarnovin MH, Jafari-Talookolaei RA, Ahmadian MT. Vibration analysis of delaminated Timoshenko beams under the motion of a constant amplitude point force traveling with uniform velocity. Int J Mech Sci 2013;70:39–49.
[28] Shariati-Nia M, Torabi K, Heidari-Rarani M. Free vibration analysis of a composite beam with single delamination – An improved free and constrained model. Eng Solid Mech 2014;2:313–20.
[29] Szekrenyes A. Coupled flexural–longitudinal vibration of delaminated composite beams with local stability analysis. J Sound Vib 2014;333(20):5141–64.
[30] Szekrenyes A. A special case of parametrically excited systems: free vibration of delaminated composite beams. Eur J Mech A/Solid 2015;49:82–105.
[31] Zhang Z, Shankar K, Ray T, Morozov EV, Tahtali M. Vibration-based inverse algorithms for detection of delamination in composites. Compos Struct 2013;102:226–36.
[32] Ihesiulor OK, Shankar K, Zhang Z, Ray T. Delamination detection with error and noise polluted natural frequencies using computational intelligence concepts. Compos Part B: Eng 2014;56:906–25.
[33] Ihesiulor OK, Shankar K, Zhang Z, Ray T. Validation of algorithms for delamination detection in composite structures using experimental data. J Compos Mater 2014;48(8):969–83.
[34] Thalapil J, Maiti SK. Detection of longitudinal cracks in long and short beams using changes in natural frequencies. Int J Mech Sci 2014;83:38–47.
[35] ASTM Standard D 3039, Standard test method for tensile properties of polymer matrix composite materials. Annual Book of ASTM Standards, 2002.
[36] ASTM Standard D 3518, Standard test method for in-plane shear response of polymer matrix composite materials by tensile test of a $\pm 45^{\circ}$ laminate. Annual Book of ASTM Standards, 2002.
[37] Torabi K, Jafarzadeh Jazi A, Zafari E. Exact closed form solution for the analysis of the transverse vibration modes of a Timoshenko beam with multiple concentrated masses. Appl Math Comput 2014;238:342–57.